Atmos. Chem. Phys. Discuss., 11, 23469–23511, 2011
www.atmos-chem-phys-discuss.net/11/23469/2011/
doi:10.5194/acpd-11-23469-2011

Atmospheric Chemistry and Physics Discussions

ANISORROPIA: the adjoint of the aerosol thermodynamic model ISORROPIA

S. L. Capps[1], **D. K. Henze**[2], **A. Hakami**[3], **A. G. Russell**[4], **and A. Nenes**[1,5]

[1]School of Chemical and Biomolecular Engineering, Georgia Institute of Technology, Atlanta, GA, USA
[2]Deparment of Mechanical Engineering, University of Colorado, Boulder, CO, USA
[3]Department of Civil and Environmental Engineering, Carleton University, Ottawa, ON, Canada
[4]School of Civil and Environmental Engineering, Georgia Institute of Technology, Atlanta, GA, USA
[5]School of Earth and Atmospheric Sciences, Georgia Institute of Technology, Atlanta, GA, USA

Received: 2 August 2011 – Accepted: 5 August 2011 – Published: 19 August 2011

Correspondence to: A. Nenes (athanasios.nenes@gatech.edu)

Published by Copernicus Publications on behalf of the European Geosciences Union.

Abstract

We present the development of ANISORROPIA, the discrete adjoint of the ISORROPIA thermodynamic equilibrium model that treats the Na^+-SO_4^{2-}-HSO_4^--NH_4^+-NO_3^--Cl^--H_2O aerosol system, and we demonstrate its sensitivity analysis capabilities. ANISORROPIA calculates sensitivities of an inorganic species in aerosol or gas phase with respect to the total concentrations of each species present with only a two-fold increase in computational time over the forward model execution. Due to the highly nonlinear and discontinuous solution surface of ISORROPIA, evaluation of the adjoint required a new, complex-variable version of the the model, which determines first-order sensitivities with machine precision and avoids cancellation errors arising from finite difference calculations. The adjoint is verified over an atmospherically relevant range of concentrations, temperature, and relative humidity. We apply ANISORROPIA to recent field campaign results from Atlanta, GA, USA, and Mexico City, Mexico, to characterize the inorganic aerosol sensitivities of these distinct urban air masses. The variability in the relationship between $PM_{2.5}$ mass and precursor concentrations shown has important implications for air quality and climate. ANISORROPIA enables efficient elucidation of aerosol concentration dependence on aerosol precursor emissions in the context of atmospheric chemical transport model adjoints.

1 Introduction

Atmospheric chemical transport models (CTMs) are used for many purposes including assessment of radiative climate forcing of aerosol (Forster et al., 2007) and evaluation of the effectiveness of emissions control strategies designed to reduce exposure of humans to particulates (EPA, 2004). The accuracy of these estimates is limited by model representations of chemical and physical processes as well as model parameters (e.g., emissions rates). Attributing climate forcing and air quality degradation to sources is challenging with sensitivity analysis techniques based on standard model output

(Shindell et al., 2008, 2009). Inorganic species, primarily sulfate ($SO^{2-}_{4(aq)}$/$HSO^{-}_{4(aq)}$), ammonium ($NH^{+}_{4(aq)}$), nitrate ($NO^{-}_{3(aq)}$), sodium ($Na^{+}_{(aq)}$), and chloride ($Cl^{-}_{(aq)}$), constitute a significant fraction of dry aerosol mass (Heintzenberg, 1989). The nonlinear formation of inorganic aerosol from gas phase precursors is reasonably well-characterized (Nenes et al., 1999). However, the precision of emissions estimates of aerosol precursors varies widely depending upon source type and region of the world (Klimont and Streets, 2007). Adjoint-based sensitivity analysis enhances the ability to assess the relative influence of aerosol precursor emissions on air quality metrics and aerosol radiative forcing of climate as well as providing a means of refining emissions estimates with observations.

The highly variable sensitivity of fine mode ammonium-sulfate-nitrate aerosol to precursor concentrations (Ansari and Pandis, 1998; West et al., 1999) challenges the robust assessment of emissions influences. West et al. (1998) demonstrated climatic implications of this variability by quantifying the marginal direct radiative forcing of inorganic aerosols. Vayenas et al. (2005) explored the relationship of $SO_{2(g)}$ and $NO_{x(g)}$ emissions to SO_4^{2-}-HSO_4^{-}-NH_4^{+}-NO_3^{-} aerosol concentrations in an observationally driven Eulerian model over the eastern United States, finding significant variation in effectiveness of controls because of the nonlinear transformation of gaseous precursors to aerosol. Pinder et al. (2007) demonstrated the efficiency of reducing $NH_{3(g)}$ emissions relative to $SO_{2(g)}$ and $NO_{x(g)}$ for air quality objectives with the PM-CAMx CTM (Gaydos et al., 2007) by perturbing emissions of $NH_{3(g)}$, $SO_{2(g)}$, and $NO_{x(g)}$ by fifty percent. Although the finite difference approach employed in this and other studies, sometimes termed "emissions toggling", is the most straightforward sensitivity analysis technique, it is limited in that computational requirements scale with the number of emissions investigated; perturbations to the atmospheric conditions from the changed emissions obscure nonlinear effects; and cancellation errors limit the accuracy of this method. The decoupled direct method (DDM), an implementation of a tangent linear model (TLM), reveals the impact of selected emissions on the field of air quality or health metrics without perturbing the model state (Dunker, 1984; Napelenok et al., 2006; Koo et al., 2007); second-order source-oriented sensitivities of inorganic aerosol can now quantify nonlinear contributions to sensitivity (Zhang et al., submitted). Establishing the source-receptor relationship of inorganic aerosol by these forward sensitivity analysis methods (i.e., emissions toggling, DDM/TLM) reveals emissions impacts of particular sources on the field of concentrations. Source-oriented sensitivity analysis is less helpful for evaluating relative impacts of emissions, and inverse modeling with source-oriented sensitivities is limited in application due to computational cost, which scales with model parameters assessed (Mendoza-Dominguez and Russell, 2001).

The adjoint method complements forward sensitivity approaches by efficiently elucidating the relationship of model output (e.g., specified concentrations, air quality metrics) to the field of model parameters (e.g., emissions, initial conditions) without perturbing model inputs or results. Computational requirements for calculation of these receptor-oriented sensitivities are insensitive to the number of model parameters investigated. Thus, adjoints can efficiently calculate sensitivities of air quality or climate-forcing metrics with respect to a vast number of parameters (e.g., 10^5) in accordance with model chemistry and physics. This receptor-oriented approach facilitates optimization of model parameters in accordance with observations in a 4-dimensional variational (4D-Var) data assimilation framework.

Meteorologists have exploited adjoints for optimization of initial conditions and other parameters for decades (Sasaki, 1958; Marchuk, 1974; Lamb et al., 1975; Talagrand, 1981; Talagrand and Courtier, 1987). CTM adjoints have been used to explore gas-phase sensitivity relationships (Menut et al., 2000; Vukićević and Hess, 2000; Sandu et al., 2005a; Hakami et al., 2006; Martien and Harley, 2006) and to refine estimates of trace gases in the atmosphere (Fisher and Lary, 1995; Elbern et al., 1997; Kaminski et al., 1999; Elbern et al., 2000; Müller and Stavrakou, 2005; Zhang et al., 2008; Kopacz et al., 2009). Gas phase 4D-Var data assimilation has been employed to improve agreement of model predictions with in situ observations (e.g., Chai et al., 2006) or remote sensing (e.g., Resler et al., 2010). Kukkonen et al. (2011) anticipate the utility of 4D-Var data assimilation of trace gas observations within a coupled meteorological-chemical forecasting model framework for real-time improvement of air quality forecasting.

Application of adjoint methods to study aerosols is relatively new, likely due, in part, to the difficulty of developing adjoints of aerosol models as well as recently increased impetus for their utility. Henze et al. (2004) and Sandu et al. (2005b) demonstrated the feasibility of developing an adjoint for the coagulation and growth of a multi-component aerosol population in a 0-D model. Hakami et al. (2005) first optimized initial and boundary conditions as well as emissions rates of non-reactive black carbon (BC) aerosol using an adjoint of the STEM-2k1 model (Carmichael et al., 2003; Sandu et al., 2005a) to assimilate in situ observations from ACE-Asia (Huebert et al., 2003; Seinfeld et al., 2004). The adjoint of GOCART, a global aerosol transport model, demonstrated the utility of satellite-based aerosol observations for constraining highly uncertain aerosol emissions parameters (Dubovik et al., 2008). The distribution and long-range transport of Asian dust have been investigated with a 4D-Var data assimilation version of a regional dust transport model (RC4) with both in situ and remotely sensed observations (Yumimoto et al., 2007, 2008; Uno et al., 2008; Sekiyama et al., 2010). The direct and albedo forcings of black carbon deposited on the Tibetan Plateau were characterized by Kopacz et al. (2011) with the adjoint of GEOS-Chem. Henze et al. (2007) first included secondary formation of inorganic aerosol in the adjoint of GEOS-Chem using MARS-A, a thermodynamic model of the SO_4^{2-}-HSO_4^--NH_4^+-NO_3^--H_2O aerosol system (Binkowski and Roselle, 2003). With this framework, Henze et al. (2009) conducted inverse modeling of inorganic fine mode aerosol observations from the IMPROVE network (Malm et al., 1994) to identify influences of aerosol precursor emissions on US air quality.

Many regional and global CTMs employ ISORROPIA/ISORROPIA-II (Nenes et al., 1998, 1999; Fountoukis and Nenes, 2007), a thermodynamic equilibrium model. ISORROPIA treats the Na^+-SO_4^{2-}-HSO_4^--NH_4^+-NO_3^--Cl^--H_2O aerosol system by efficiently and accurately calculating the partitioning of precursor gases and water vapor to aerosol at a specified temperature and relative humidity (RH). ISORROPIA simulates secondary inorganic aerosol formation in CHIMERE (Schmidt et al., 2001; Bessagnet et al., 2004), Community Multiscale Air Quality model (CMAQ) (Byun and Schere, 2006), Comprehensive Air Quality Model with Extensions (CAMx) (ENVIRON, 1997, 2010), COSMO-ART (Vogel et al., 2009), GEOS-Chem (http://geos-chem.org/) (Bey et al., 2001; Pye et al., 2009), LOng Term Ozone Simulation–EURopean Operational Smog model (LOTOS-EUROS) (Schaap et al., 2008), and the Sulfur Transport dEposition Model (STEM-2k1) (Carmichael et al., 2003). Although ISORROPIA is capable of treating the entire deliquescence curve, these CTMs often approximate the aerosol as metastable solutions due to the high probability of residual water existing in the aerosol.

Receptor-oriented sensitivity analysis and inverse modeling have been limited to gaseous species or inert aerosol for CTMs that employ ISORROPIA due to the absence of its adjoint, which this work addresses. We present the development of ANISORROPIA (AdjoiNt of ISORROPIA) (Sect. 2), demonstrate its accuracy at atmospherically relevant conditions (Sect. 3), and apply it to examine observed aerosol mixture responses (Sect. 4). Finally, the utility of ANISORROPIA for conducting sensitivity analysis and inverse modeling within adjoints of CTMs is thoroughly discussed (Sect. 5).

2 Methods

The adjoint of a CTM determines sensitivities of a metric of specified output parameters (e.g., air quality attainment metric) with respect to a wide array of input parameters (i.e., emissions rates). Conceptually, an infinitesimal variation in a single output variable evolves backwards through modeled processes to produce a field of requisite perturbations in the input parameters. Realizing this capability in a CTM with an online simulation of aerosol involves considerable methodological and coding development. Outlined in the following sections are the mathematical framework for sensitivity analysis and inverse modeling (Sect. 2.1), the role of ISORROPIA in CTMs (Sect. 2.2), and the specific tactics employed to develop ANISORROPIA (Sect. 2.3).

2.1 Mathematical background

CTMs model the concentrations of atmospheric species in time and space in accordance with meteorological conditions; emissions rates, initial conditions, and boundary conditions are requisite model parameters for solution of the system of partial differential equations forming the model. The complexity of the system obscures the effects of model parameters, $\boldsymbol{p}$, on a modeled concentration, c, or a concentration-dependent metric, $g(\boldsymbol{c})$, such as the radiative forcing of a modeled species or mortality as a function of concentration. Sensitivity analysis with model adjoints can efficiently unravel these complex dependencies by calculating $\nabla_{\boldsymbol{p}}\boldsymbol{J}$ for

$$\boldsymbol{J} = \sum_{g\epsilon\Omega_{\mathrm{s}}} g(\boldsymbol{c}) \tag{1}$$

where Ω_{s} is the set of cost function evaluations in time and space (Henze et al., 2007). For example, a CTM adjoint could reveal the relative influence on a non-attainment air quality metric of each emissions parameter with resolution in source type, time, and space. The adjoint of each modeled chemical and physical process defines the receptor-oriented sensitivity; therefore, the aerosol thermodynamic equilibrium model employed in the forward model must also be employed in the adjoint to characterize sensitivities consistently.

To conduct 4D-Var data assimilation, the cost function, $\boldsymbol{J}$ is defined as the level of agreement between modeled and observed values. Rodgers (2000) and Henze et al. (2007) explain the variational framework in detail; thus, this discussion is limited to that necessary to understand advantages achieved with the adjoint approach to inverse modeling. In the 4D-Var framework, observations of modeled species are assimilated by evaluation of a two-part cost function, which weights the difference of modeled concentrations translated into observation space, $\mathcal{H}(\boldsymbol{c})$, from observations, $\boldsymbol{c}^{\mathrm{obs}}$, and the deviation of optimized model parameters, $\boldsymbol{p}$, from the a priori value, $\boldsymbol{p}_a$ (Eq. 2)

$$J = \frac{1}{2}\sum_{c\epsilon\Omega}(\mathcal{H}(c) - c^{\text{obs}})^T\mathbf{R}^{-1}(\mathcal{H}(c) - c^{\text{obs}}) + \frac{1}{2}\gamma(p - p_a)^T\mathbf{B}^{-1}(p - p_a) \qquad (2)$$

where **R** denotes the observational error covariance matrix; **B** denotes the a priori value of the model covariance matrix; and γ denotes the regularization parameter, which controls the extent to which observations or a priori estimates constrain the solution (Rodgers, 2000). Typically, the value of the cost function is minimized by a gradient-based algorithm, which leads to the evaluation of $(\nabla_{\boldsymbol{p}}F)^T\mathbf{R}^{-1}(\mathcal{H}(\boldsymbol{c}) - \boldsymbol{c}^{\text{obs}})$, where $\nabla_{\boldsymbol{p}}F$ represents the Jacobian of the model. The TLM of a CTM, a source-oriented sensitivity analysis method, can be employed to form the Jacobian, which can be transposed to achieve the solution to (Eq. 2). This approach has been taken for trace gases with observations from ground-based measurements (e.g., Mendoza-Dominguez and Russell, 2001), flight-based measurements (e.g., Streets et al., 2006), and satellite observations (e.g., Kaynak et al., 2009); however, the large dimensionality of the Jacobian and the number of observations limits the number of parameters that can be optimized in this manner.

Adjoint-based evaluation of the gradient of the cost function is unconstrained by the number of model parameters; the model adjoint, $(\nabla_{\boldsymbol{p}}F)^T$, directly operates on $\mathbf{R}^{-1}(\mathcal{H}(\boldsymbol{c}) - \boldsymbol{c}^{\text{obs}})$, which is termed the adjoint forcing vector. Thus, the Jacobian need not be formed to minimize the cost function. The gradient is accumulated from the final observation time back to the start of the time period of interest, yielding efficient calculation of $\nabla_{\boldsymbol{p}}\boldsymbol{J}$. The cost function is iteratively minimized as the gradient-based minimization routine adjusts the model parameters in accordance with $\nabla_{\boldsymbol{p}}\boldsymbol{J}$. Therefore, the computational burden scales with the number of cost functions evaluated rather than the number of input variables optimized (i.e., length($\boldsymbol{p}$)). For example, the adjoints of GOCART and GEOS-Chem have been employed to optimize significant numbers ($\sim 10^5$) of emissions parameters affecting aerosol concentrations with computational effort comparable to the forward model execution (e.g., Dubovik et al., 2008; Henze et al., 2009). These model adjoints lacked comprehensive thermodynamic modeling, which is enabled by ISORROPIA/ANISORROPIA.

2.2 The ISORROPIA model

Key components of fine mode aerosol are water, inorganic salts, crustal minerals, organics, and trace metals (Seinfeld and Pandis, 2006). Inorganic species constitute about 25–50 % of the dry mass of a typical continental particle, the most abundant being sulfate ($SO^{2-}_{4(aq)}$/$HSO^{-}_{4(aq)}$), ammonium ($NH^{+}_{4(aq)}$), and nitrate ($NO^{-}_{3(aq)}$). Sodium ($Na^{+}_{(aq)}$) and chloride ($Cl^{-}_{(aq)}$) ions contribute significantly in environments with marine character or near dry lake beds (Heintzenberg, 1989). The timescale of equilibration for fine mode aerosol is generally less than twenty minutes, which supports the treatment of these particles in CTMs as existing in thermodynamic equilibrium with the surrounding gases (Ansari and Pandis, 1999b; Dassios and Pandis, 1999; Fountoukis et al., 2009).

A number of thermodynamic models have been developed to model aerosol thermodynamic equilibrium with varying degrees of comprehensiveness, accuracy, and efficiency (e.g., AIM (Clegg et al., 1998); GFEMIN (Ansari and Pandis, 1999a); EQSAM3 (Metzger et al., 2006; Metzger and Lelieveld, 2007); EQUISOLV II (Jacobson et al., 1996; Jacobson, 1999); ISORROPIA and ISORROPIA II (Nenes et al., 1998, 1999; Fountoukis and Nenes, 2007); MARS-A (Saxena et al., 1986; Binkowski and Roselle, 2003); MESA (Zaveri et al., 2005); SCAPE2 (Kim et al., 1993a,b; Meng and Seinfeld, 1996); UHAERO (Amundson et al., 2006)).

Until now, the adjoint of one thermodynamic equilibrium model has been developed: RPMARES, an implementation of the MARS-A model for GEOS-Chem (Binkowski and Roselle, 2003; Park et al., 2004; Henze et al., 2007). RPMARES treats the ammonium-sulfate-nitrate aerosol system with temperature-independent activity coefficients based on the Pitzer model for binary coefficients. ISORROPIA treats two additional species, sodium and chloride, and includes temperature dependence when calculating activity coefficients by the Kusik-Meissner (K-M) method. K-M reproduces experimental results as well as or better than the Pitzer model (Kim et al., 1993b). In ISORROPIA, water uptake is calculated in accordance with AIM Model III (http://www.aim.env.uea.ac.uk/aim/aim.php) rather than older data sets (Binkowski and Roselle, 2003; Fountoukis and Nenes, 2007). Inclusion of additional species, increased accuracy compared to RPMARES, and widespread utilization of ISORROPIA in CTMs motivated development of ANISORROPIA.

ISORROPIA solves the aerosol-gas partitioning problem in two different modes: forward and reverse. Model input for the forward mode is the total amount of species present in the gas and aerosol; it outputs the gas phase and aerosol concentrations of each of the species. The reverse mode requires the concentration of species in the aerosol and calculates gas phase concentrations of species in equilibrium. The focus of the current work is the forward mode as it is more widely employed. The reverse mode is useful for aerosol dynamics codes with active mass transfer of aerosol species (e.g., Capaldo et al., 2000; Pilinis et al., 2000; Kelly et al., 2010).

ISORROPIA uses ten distinct algorithms to determine equilibrium based on the relative abundance of negatively and positively charged ionic species (i.e., the acidity of the aerosol) for the NH_4^+-SO_4^{2-}-HSO_4^--NO_3^--Na^+-Cl^--H_2O aerosol system. The sulfate ratio, $R_S = \frac{[\text{Total NH}_3]+[\text{Total Na}]}{[\text{Total H}_2\text{SO}_4]}$, determines which solution branch is employed. For $R_S \geq 2$, the neutralized solution regime is accessed since sufficient ammonium and sodium are present to neutralize the aerosol sulfate. $R_S < 2$ invokes one of the seven acidic solution algorithms. Discretization of the solution space reduces the computational complexity and increases efficiency of determining equilibrium of a multicomponent system; therefore, ANISORROPIA was designed to be congruent with the underlying model.

2.3 Development of ANISORROPIA

Accumulation of adjoint sensitivities occurs through a set of calculations which parallel the original model; a model adjoint can be formed in one of two ways. If the governing equations are differentiated and then transformed into a numerical algorithm, the adjoint is termed a continuous adjoint; hence, the discretization of the adjoint model may not be in accordance with the underlying model. Conversely, a discrete adjoint is formed by the differentiation of the forward model in accordance with the original model algorithm. Automatic differentiation (AD) tools, which apply the chain rule line by line, can be efficiently employed as aids to discrete adjoint development (http://www.autodiff.org/); alternately, the discrete adjoint can be formed by hand.

A discrete adjoint is developed to maintain consistency with the model and because the efficiency of ISORROPIA largely arises from the discretization of the solution space. ANISORROPIA has been developed for each of the ten solution regimes involved in the forward mode for the deliquesced NH_4^+-SO_4^{2-}-HSO_4^--NO_3^--Na^+-Cl^--H_2O aerosol system. The appropriate solution regime is accessed according to the relative abundance of total species present. An internal driver calls the appropriate adjoint routine based on the acidity of the aerosol, which is consistent with that executed by the forward model. ANISORROPIA does not checkpoint the solution regime called during the forward execution of ISORROPIA because a simple arithmetic calculation from input to ANISORROPIA is sufficient to select the appropriate solution pathway.

Within each of the ten solution pathways, ISORROPIA remains sufficiently complex that writing the adjoint of this FORTRAN code by hand would be very challenging. The high degree of interdependence in addition to the length of the code (~10 000 lines) made employing an AD tool an attractive alternative. TAPENADE, an AD tool for FORTRAN and C programs (Hascoët and Pascual, 2004), was used to augment the forward model with sensitivity calculations capable of treating adjoint forcing vectors provided in a box modeling context or passed from other parts of a CTM adjoint. ISORROPIA originally calculated activity coefficients to single-precision; development of ANISORROPIA required conversion of all variables to double-precision to accumulate sensitivities through this aspect of the model accurately.

ANISORROPIA input includes total concentrations, temperature, and RH as well as the adjoint forcing vector, the elements of which correspond exactly to the output arrays of ISORROPIA (i.e., aqueous and gaseous partitioned-species concentrations). In ANISORROPIA execution, branches and iterations are noted with inexpensive variable accumulation, and variable values are temporarily stored in memory during the forward calculations (Fig. 1, blue lines); then, the same procedures are executed in reverse order while accumulating gradients in corresponding sensitivity calculations driven by the forcing vector (Fig. 1, orange lines). Thus, ANISORROPIA produces partial derivatives of the output species indicated in the forcing vector with respect to each input species (i.e., sum of aqueous and gaseous species concentration). If the adjoint forcing vector is null except for a single element equal to unity, ANISORROPIA produces the row of the Jacobian of ISORROPIA corresponding to the element equal to unity; for instance, if the element of the adjoint forcing vector corresponding to $[\mathrm{NH}^+_{4(aq)}]$ is unity and all others zero, ANISORROPIA produces the array $\frac{\partial[\mathrm{NH}^+_{4(aq)}]}{\partial[\mathbf{X}]}$, where $[X]$ is the array of concentrations of the sum of the aqueous and gaseous forms of species X, one of the total species tracked by ISORROPIA. Forward sensitivity analysis methods produce the column of the Jacobian corresponding to a selected $[X]$; hence, a single execution of a forward sensitivity analysis method could yield the array $\frac{\partial[\mathbf{Y}]}{\partial[\mathrm{Total\,H_2SO_4}]}$, where $[\mathbf{Y}]$ is the array of concentrations of partitioned species, Y. In this way, the Jacobian produced by ANISORROPIA can be compared directly to that determined by a forward sensitivity analysis method for model evaluation.

For acidic cases (i.e., $R_S < 2$), ISORROPIA iteratively resolves activity coefficients to convergence. The iterative nature of the forward solution is maintained in the adjoint of the acidic cases (Fig. 1a). Straightforward manipulation of ISORROPIA code was required to indicate which sensitivities should be traced by TAPENADE. The only modification to the forward solution is to increase the precision with which activity coefficients are calculated so that accurate sensitivity calculations can be obtained.

In the case of neutralized aerosol (i.e., $R_S \geq 2$), ISORROPIA evaluates whether equilibrium has been achieved by a selected saturation ratio. For instance, in the NH_4^+-SO_4^{2-}-HSO_4^--NO_3^--H_2O aerosol system, all equations are solved successively so that only one equilibrium needs to be numerically solved, namely $NH_{3(g)} + H_2O_{(aq)} \leftrightharpoons NH^+_{4(aq)} + OH^-_{(aq)}$; therefore, satisfactory equilibrium is achieved when $\frac{[NH^+_{4(aq)}][OH^-_{(aq)}]}{K[NH_{3(g)}]} = 1$, where $[X]$ denotes the concentration of species X in mol m^{-3} and K denotes the relevant equilibrium constant. Across the range of potential partitioned concentrations, the saturation ratio closely approximates the behavior of a step function owing to the very large change in species partitioning with small shifts in pH. The stability of the bisection method ensures convergence to the root of $\frac{[NH^+_{4(aq)}][OH^-_{(aq)}]}{K[NH_{3(g)}]} = 1$ in ISORROPIA. The discontinuous nature of this algorithm required modification of the underlying model in order for sensitivities to be traced through the solution. For $R_S \geq 2$ in the NH_4^+-SO_4^{2-}-HSO_4^--H_2O aerosol system, a stable method of iterating to convergence of activity coefficients, as employed for $R_S < 2$ cases, was developed. For the neutralized cases in the NH_4^+-SO_4^{2-}-HSO_4^--NO_3^- and NH_4^+-SO_4^{2-}-HSO_4^--NO_3^--Na^+-Cl^--H_2O aerosol systems, the post-convergence Newton-Raphson (N-R) method was implemented (Bartholomew-Biggs, 1998) (Fig. 1b). Gradients required by N-R are calculated with TAPENADE-produced TLMs of the function being treated by bisection; that is, the chain rule is applied line-by-line to produce the sensitivity of the equilibrium equation of interest (e.g., $\frac{[NH^+_{4(aq)}][OH^-_{(aq)}]}{K[NH_{3(g)}]} = 1$) with respect to its input (e.g., moles of $NH_{3(g)}$ partitioning to the aerosol). After bisection, one iteration of the N-R method is evaluated. By adding a differentiable calculation subsequent to the original algorithm, the stability of the bisection algorithm is maintained while providing the functionality necessary for adjoint calculations. It is sufficient to take the adjoint of this single step (Bartholomew-Biggs, 1998). A stringent convergence criterion must be employed to ensure that the numerical solution of the bisection method is not modified in the N-R step. The error system of ISORROPIA is augmented to note when bisection does not sufficiently converge to enable accurate N-R calculation; the forward and adjoint codes return this flag for appropriate treatment by the host model.

3 Evaluation of ANISORROPIA

A two-part evaluation of ANISORROPIA was conducted. First, the partitioned concentrations given by ANISORROPIA were evaluated against ISORROPIA v.2.1 for an atmospherically relevant range of RH (5–95 %), temperature (288–308 K), and total concentrations to ensure that the forward calculations are not altered by the modifications of the code required to calculate the adjoint derivatives. total concentrations ranges were 1–50 $\mu g\, m^{-3}$ H_2SO_4; 0.2–9 $\mu g\, m^{-3}$ NH_3; 0–16 $\mu g\, m^{-3}$ HNO_3; 0–18 $\mu g\, m^{-3}$ Na; and 0–30 $\mu g\, m^{-3}$ HCl. Approximately 450 000 sets of model input were evaluated of which 70 % ANISORROPIA processed without producing an error code indicating that convergence could not be reached (Fig. 2). The stiffness of the numerical solution for equilibrium at high ionic concentrations due to the metastable assumption sometimes leads to insufficient convergence for accurate adjoint sensitivity calculation. For the convergent cases, ANISORROPIA concentrations are less than 0.1 % different than results of the modified ISORROPIA v2.1 (Fig. 2, $R^2 = 1.00$). Having ensured that the sensitivities would be evaluated for nearly identical simulated equilibrium concentrations, the accuracy of the adjoint sensitivities was assessed by comparison to sensitivities calculated using the complex variable method.

3.1 The complex variable method

The truncated Taylor series expansion of $F(x)$ about a point (x_0) leads to the central finite difference approximation of $\frac{\partial F}{\partial x}$ with truncation error $O(h^2)$ given by

$$\frac{\partial F}{\partial x} = \lim_{h \to 0} \frac{F(x_0 + \frac{1}{2}h) - F(x_0 - \frac{1}{2}h)}{h} \quad (3)$$

where F is a real analytic function and h is a small, real perturbation. Lyness and Moler (1967) demonstrated that complex numbers are useful for numerical approximation of derivatives; however, the number of calculations required for their approach, based on Cauchy's integral theorem, limited application of the technique (Lantoine et al., 2010). Squire and Trapp (1998) developed an efficient complex step differentiation method which maintains machine precision in the derivative. For the complex analytic function $G(z)$, where z is a complex argument, an analogous expression for $\frac{\partial G}{\partial z}$ with approximation error $O(h^2)$ arises:

$$\frac{\partial G}{\partial z} = \lim_{h \to 0} \frac{\mathrm{Im}[G(z_0 + ih)]}{h} \tag{4}$$

where $i = \sqrt{-1}$ and Im selects the imaginary part of the argument (Squire and Trapp, 1998). The complex variable method (CVM) as introduced by Squire and Trapp (1998) eliminates subtraction cancellation and numerical round-off errors, the primary difficulties of numerical differentiation (Lyness and Moler, 1967).

To implement CVM in a FORTRAN-based numerical model such as ISORROPIA, variables are declared as COMPLEX rather than REAL, and intrinsic functions are modified to treat complex arguments (Giles and Pierce, 2000). This conversion is straightforward with the exception of the functions that must be approximated to accept COMPLEX arguments, such as the arccosine function, ACOS. ACOS is called within the analytical solution of the cubic polynomial $x^3 + A_1 x^2 + A_2 x + A_3 = 0$. CVM requires that the sensitivity accumulate through this function without being altered by calculations in the imaginary part due to $\frac{\partial x_0}{\partial A_i} = \frac{\mathrm{Im}(x_0)}{\mathrm{Im}(A_i)}$ where x_0 is the desired solution of the cubic polynomial and A_i represents the coefficients of the polynomial. Rather than using an alternate analytical solution to avoid calling ACOS, the imaginary part of x_0 was calculated independently. To do so, $\mathrm{Im}(A_i)$ were stored, and the desired real root calculated by the original function operating only on the real parts of A_i. The analytical total derivative of the cubic polynomial gives

$$\mathrm{Im}(x_0) = \frac{-x_0^2 \times \mathrm{Im}(A_1) - x_0 \times \mathrm{Im}(A_2) - \mathrm{Im}(A_3)}{3x_0^2 + 2A_1 x_0 + A_2} \tag{5}$$

by which $\mathrm{Im}(x_0)$ is obtained. This strategy is readily applicable in other CVM applications to similar calculations involving functions that must be approximated to treat a complex argument.

3.2 Sensitivity comparison

Although the accuracy of finite difference sensitivities is limited by round-off error, nonlinear effects, and solution discontinuities, these provide the most straightforward method of evaluating partial derivatives calculated by adjoints (Giles and Pierce, 2000); therefore, adjoint-based sensitivities are typically compared to those from the central finite difference method (e.g., Martien et al., 2006; Henze et al., 2007; Hakami et al., 2007). The highly nonlinear, discontinuous solution surface of ISORROPIA and associated subtraction cancellation errors rendered this method ineffective as demonstrated in evaluation against CVM results. For example, finite difference sensitivities of aqueous sulfate to total sulfate exceeded stoichiometric expectations for the same input for which the CVM found reasonable sensitivities (Fig. 3). To overcome this issue, CVM is used for evaluation of ANISORROPIA sensitivities.

The adjoint sensitivities from ANISORROPIA are compared to those from CVM over the same evaluation range which was employed for the concentrations described in Sect. 3.1 (Fig. 4) as well as over a lower temperature range (268–288 K, not shown). Thirty-five sensitivities of the aerosol concentration (model output: $\mathrm{Cl}^-_{(aq)}$, $\mathrm{H}^+_{(aq)}$, $\mathrm{HSO}^-_{4(aq)}$, $\mathrm{Na}^+_{(aq)}$, $\mathrm{NH}^+_{4(aq)}$, $\mathrm{NO}^-_{3(aq)}$, $\mathrm{SO}^{2-}_{4(aq)}$) to the sum of gaseous and aerosol concentrations (model input: total chloride, total nitrate, total sulfate, total ammonium, and total sodium) were evaluated for each of the aqueous aerosol species with respect to each aerosol precursor as these are the gradients required by the CTM adjoints.

Testing other sensitivities (e.g., gaseous concentration with respect to total species) is also possible but redundant. The ANISORROPIA-produced sensitivities are compared against CVM results (Fig. 4). The black solid line represents $y = x$ and depicts the region of perfect agreement; approximately 10^6 points are represented in each of the six sensitivity comparisons. Excellent agreement in the results verifies that the adjoint sensitivities are consistent with the model sensitivities.

3.3 Computational efficiency

The computational time required for execution of ANISORROPIA forward and adjoint sensitivity calculations was assessed by comparing the elapsed CPU time against ISORROPIA v.2.1 with a double-precision activity coefficient module. Both models were executed with the same convergence criteria (i.e., relative difference of activity coefficients from previous iteration $< 10^{-10}$). Model input ranges were designed to examine the three different aerosol systems individually. All written output was suppressed so that calculations, not variable writing processes, were evident in the comparisons. The assessment was conducted on a 2.93 GHz Intel Core i7 processor running Mac OS X v10.6; source code was compiled with O3 optimization by the Intel Fortran compiler. The adjoint never exceeds a three-fold increase in computational time over the original model (Fig. 5), which is far less than the theoretical upper limit of a factor of five (Griewank, 1989).

The atmospherically relevant evaluation range (Sect. 3.1) bounded the input for the timing experiments. For the NH_4^+-SO_4^{2-}-HSO_4^--H_2O aerosol system, modifications necessary for the adjoint calculations caused an almost negligible increase in computational time. Moderate (20 % or less) increases in forward calculation computational time were from modifications for the NH_4^+-SO_4^{2-}-HSO_4^--NO_3^--H_2O and NH_4^+-SO_4^{2-}-HSO_4^--NO_3^--Na^+-Cl^--H_2O aerosol systems. The efficiency of the adjoint of the post-convergence N-R method is evident since the increase in computational time is least for the NH_4^+-SO_4^{2-}-HSO_4^--NO_3^--H_2O and NH_4^+-SO_4^{2-}-HSO_4^--NO_3^--Na^+-Cl^--H_2O aerosol systems in which it was employed. These conditions are far more abundant in the atmosphere than the NH_4^+-SO_4^{2-}-HSO_4^- system. ANISORROPIA requires similar increases in computational time as the gas-phase adjoint of CMAQ and the adjoint of GEOS-Chem, which are 2 and 1.5 times the original model, respectively (Hakami et al., 2007; Henze et al., 2007). As for memory requirements, the only values necessary from the adjoint forward execution are total species concentrations, RH, and temperature; all values needed for adjoint calculations are recomputed or stored internally in allocatable arrays using the efficient PUSH/POP mechanism of TAPENADE (Hascoët and Pascual, 2004).

4 Application

ANISORROPIA has been developed for application within the adjoints of CTMs from regional (e.g., Community Multiscale Air Quality model (CMAQ), Byun and Schere, 2006) to global scales (e.g., GEOS-Chem, Henze et al., 2007); in these frameworks, its potential can be fully realized. Nevertheless, applied independently of a CTM, ANISORROPIA provides an efficient, reliable method of determining the sensitivity of dry, inorganic fine mode aerosol to changes in total concentration of sulfate, ammonia, nitrate, sodium, and chloride for deliquesced aerosol. The input required is exactly the same as the forward mode of ISORROPIA (i.e., total concentrations, RH, temperature). ANISORROPIA is used to identify sensitivity regimes over a broad range of atmospherically relevant concentrations (Sect. 4.1). Then, conditions from in situ measurements of the inorganic composition of aerosols and quantities of the gas phase precursors $NH_{3(g)}$, $HNO_{3(g)}$, and $HCl_{(g)}$ from two distinct urban environments (Atlanta, Georgia, USA, and Mexico City, D.F., Mexico) are processed to characterize the urban $PM_{2.5}$ responsiveness to anthropogenically emitted species (Sect. 4.2).

4.1 Sensitivity regimes

ANISORROPIA is applied to produce sensitivities for the partitioning of $NH_{3(g)}$ in response to the addition of $H_2SO_{4(g)}$ and then for fine mode, dry aerosol (i.e., $PM_{2.5}$) in response to the same at 300 K (Fig. 6). Throughout much of the atmosphere, ammonium neutralizes aerosol acidity (Seinfeld and Pandis, 2006). The condensation of two moles of $NH_{3(g)}$ for each additional mole of $H_2SO_{4(g)}$ in an air parcel can be expressed as $\frac{\partial[\mathrm{NH}^+_{4(aq)}]}{\partial[\mathrm{Total\,H_2SO_4}]} = 2\,\mathrm{mol\,mol^{-1}}$. At 40 % RH, the $\frac{\partial[\mathrm{NH}^+_{4(aq)}]}{\partial[\mathrm{Total\,H_2SO_4}]}$ given by ANISORROPIA clearly reveals this behavior (Fig. 6b). Once the aerosol sulfate is neutralized, $\frac{\partial[\mathrm{NH}^+_{4(aq)}]}{\partial[\mathrm{Total\,H_2SO_4}]} = 0\,\mathrm{mol\,mol^{-1}}$ whether significant water is present (Fig. 6a) or not (Fig. 6b). In the presence of $HNO_{3(g)}$ and enough water for it to partition significantly to aerosol, $\frac{\partial[\mathrm{NH}^+_{4(aq)}]}{\partial[\mathrm{Total\,H_2SO_4}]}$ ranges between zero and two reflecting the buffering effect of $HNO_{3(g)}$, which evaporates from the aerosol as the $H_2SO_{4(g)}$ condenses (Fig. 6a). For the NH_4^+-SO_4^{2-}-HSO_4^--NO_3^--H_2O aerosol system, ANISORROPIA reveals three sensitivity regimes for $\frac{\partial[\mathrm{NH}^+_{4(aq)}]}{\partial[\mathrm{Total\,H_2SO_4}]}$.

ANISORROPIA results elucidate the dry aerosol mass changes due to the addition of 1 µg $H_2SO_{4(g)}$ at 90 % and 40 % RH. $\frac{\partial(\mathrm{PM}_{2.5,dry})}{\partial(\mathrm{Total\,H_2SO_4})}$, where (X) is the mass-based concentration of species X, ranges from 0.75 µg $(\mu g)^{-1}$ to slightly greater than 1.5 µg $(\mu g)^{-1}$. The molecular weights of sulfate (98 g $\mathrm{mol^{-1}}$), ammonium (18 g $\mathrm{mol^{-1}}$), and nitrate (62 g $\mathrm{mol^{-1}}$) are important for understanding these results. Adding one µg of sulfate to a neutralized aerosol should cause an equivalent increase in the dry aerosol mass (Fig. 6c,d). Given that acidic aerosol at lower RH has $\frac{\partial[\mathrm{NH}^+_{4(aq)}]}{\partial[\mathrm{Total\,H_2SO_4}]} = 2\,\mathrm{mol\,mol^{-1}}$, the condensation of $NH_{3(g)}$ and $H_2SO_{4(g)}$ govern the $\frac{\partial(\mathrm{PM}_{2.5,dry})}{\partial(\mathrm{Total\,H_2SO_4})}$ of 1.37 µg $(\mu g)^{-1}$ (Fig. 6d). When aerosol nitrate buffers the system by evaporation upon condensation of $H_2SO_{4(g)}$, $\frac{\partial(\mathrm{PM}_{2.5,dry})}{\partial(\mathrm{Total\,H_2SO_4})}$ drops below 1 µg $(\mu g)^{-1}$, in part due to the higher molecular weight of nitrate than ammonium, as shown in a small region of Fig. 6c. Low temperatures (~250 K) and high concentrations of total nitrate relative to total ammonium and sulfate lead to negative values of $\frac{\partial(\mathrm{PM}_{2.5,\mathrm{dry}})}{\partial(\mathrm{Total\ H_2SO_4})}$ (not shown). This variability underscores the importance of sensitivity analysis for air quality.

ANISORROPIA results for the $\mathrm{NH_4^+}$-$\mathrm{SO_4^{2-}}$-$\mathrm{HSO_4^-}$-$\mathrm{NO_3^-}$-$\mathrm{Na^+}$-$\mathrm{Cl^-}$-$\mathrm{H_2O}$ aerosol system reveal even more complex sensitivity relationships quite clearly (Fig. 7). $\frac{\partial[\mathrm{NH^+_{4(aq)}}]}{\partial[\mathrm{Total\ H_2SO_4}]}$ is shown for a system with 30 $\mu\mathrm{g\,m^{-3}}$ total HCl and 0.63 $\mu\mathrm{g\,m^{-3}}$ total $\mathrm{HNO_3}$ at 40 % RH and 300 K. The abscissa corresponds to the sum of the total amounts of the species producing positive ions, Na and $\mathrm{NH_3}$. The ordinate corresponds to the total $\mathrm{H_2SO_4}$ in the system. Region I (forward-slanted hash marks), where Na is absent, demonstrates the primary role of $\mathrm{NH^+_{4(aq)}}$ in neutralizing $\mathrm{SO^{2-}_{4(aq)}}$. The sensitivity of 2 $\mathrm{mol\,mol^{-1}}$ for $\frac{\partial[\mathrm{NH^+_{4(aq)}}]}{\partial[\mathrm{Total\ H_2SO_4}]}$ persists when $R_S \geq 2$; however, if $R_S < 2$, $\frac{\partial[\mathrm{NH^+_{4(aq)}}]}{\partial[\mathrm{Total\ H_2SO_4}]} = 0$. This behavior is consistent with that demonstrated in the $\mathrm{NH_4^+}$ -$\mathrm{SO_4^{2-}}$-$\mathrm{HSO_4^-}$-$\mathrm{NO_3^-}$-$\mathrm{H_2O}$ system (Fig. 6). Region II (vertical hash marks) reveals the system sensitivity when $\mathrm{Na^+_{(aq)}}$ contributes to neutralizing $\mathrm{SO^{2-}_{4(aq)}}$. At the far left edge of Region II, $\mathrm{Na^+_{(aq)}}$ constitutes the majority of the positive ions; therefore, the $\frac{\partial[\mathrm{NH^+_{4(aq)}}]}{\partial[\mathrm{Total\ H_2SO_4}]}$ is negligible. Moving to the right across Region II, $\mathrm{Na^+_{(aq)}}$ reaches its full potential to the neutralize $\mathrm{SO^{2-}_{4(aq)}}$, and $\frac{\partial[\mathrm{NH^+_{4(aq)}}]}{\partial[\mathrm{Total\ H_2SO_4}]}$ increases correspondingly. Finally, in Region III, the same reduced value of $\frac{\partial[\mathrm{NH^+_{4(aq)}}]}{\partial[\mathrm{Total\ H_2SO_4}]}$ appears with a dampened rate of increase of $\mathrm{NH^+_{4(aq)}}$ neutralization due to the large contribution from $\mathrm{Na^+_{(aq)}}$ and minor buffering by $\mathrm{NO^-_{3(aq)}}$ and $\mathrm{Cl^-_{(aq)}}$. ANISORROPIA could also be applied at different RH, temperature, or composition to reveal similarly meaningful sensitivity regimes.

Title Page
Abstract | Introduction
Conclusions | References
Tables | Figures
◄| |►
◄ ►
Back | Close
Full Screen / Esc
Printer-friendly Version
Interactive Discussion

4.2 Observed conditions

4.2.1 Atlanta, Georgia, USA

The Atlanta Aerosol Nucleation and Real-Time Characterization Experiment (Atlanta-ANARChE) in July and August of 2002 included measurements of $NH_{3(g)}$ and $HNO_{3(g)}$ via two distinct methods of chemical ionization mass spectrometry (Neuman et al., 2003; Nowak et al., 2006). The ground campaign was conducted at Jefferson Street in midtown Atlanta, one of the sites of the ongoing Southeast Aerosol Research and Characterization (SEARCH) study (Hansen et al., 2003) and the location of the Atlanta Supersite (Solomon et al., 2003). SEARCH instrumentation measured sulfate ($SO^{2-}_{4(aq)}$), ammonium ($NH^{+}_{4(aq)}$), and nitrate ($NO^{-}_{3(aq)}$) concentrations with continuous 1-min resolution coincident with the gas phase measurements (Edgerton et al., 2006). Meteorological data collected include RH and temperature. Nowak et al. (2006) demonstrated the accuracy of ISORROPIA in predicting the partitioned concentrations; therefore, ANISORROPIA should elucidate the aerosol sensitivities accurately.

ANARChE data were collected in the range of 25–99% RH and 293–310 K. Results find that $\frac{\partial[NH^{+}_{4(aq)}]}{\partial[\text{Total}\,H_2SO_4]} = 2\,\text{mol}\,\text{mol}^{-1}$ while the molar composition is 5–20 % total H_2SO_4 and 60–95 % Total HNO_3 (Fig. 8a). $\frac{\partial[NH^{+}_{4(aq)}]}{\partial[\text{total}\,H_2SO_4]}$ is negligible when total H_2SO_4 makes up 10–20 % and total HNO_3 makes up 20–40 % of the molar composition, which is consistent with sensitivities shown in Fig. 6a,b. The calculated $\frac{\partial(PM_{2.5,\text{dry}})}{\partial(\text{Total}\,H_2SO_4)}$ typically exceeds 1.3 µg (µg)$^{-1}$ for this time period. Condensation of $NH_{3(g)}$ to neutralize $H_2SO_{4(g)}$ occurs; additionally, sufficient $NH_{3(g)}$ is present with high concentrations of $HNO_{3(g)}$ to allow $\frac{\partial(PM_{2.5,\text{dry}})}{\partial(\text{Total}\,H_2SO_4)}$ to exceed 1.37 µg (µg)$^{-1}$ by the formation of deliquesced ammonium nitrate aerosol. When the sulfate is neutralized, $\frac{\partial(PM_{2.5,\text{dry}})}{\partial(\text{Total}\,H_2SO_4)}$ decreases to one as the addition of sulfate leads only to its condensation, not that of $NH_{3(g)}$.

4.2.2 Mexico City, D.F., Mexico

Comprehensive measurements from the Megacity Initiative: Local and Global Research Observations (MILAGRO) campaign during March of 2006 (Molina et al., 2010) facilitate the characterization of aerosol sensitivities for a very different urban air mass than that found in Atlanta due to the presence of sodium and chloride as well as significantly higher $NH_{3(g)}$ concentrations. The campaign included three ground sites with one in the urban center at the Instituto Mexicano del Petróleo (T0 site), another at the Universidad Tenológica de Tecámac in the state of Mexico (T1 site), and a third site at Rancho La Bisnaga in the state of Hidalgo (T2 site). For this investigation, data are analyzed for the period of 21–30 March 2006, from the T1 site, which is typically downwind of Mexico City. Measurements provide the $PM_{2.5}$ concentrations of $SO_{4(p)}$, $NH_{4(p)}$, $NO_{3(p)}$, $Na_{(p)}$, $Cl_{(p)}$, $Ca_{(p)}$, $K_{(p)}$, and $Mg_{(p)}$; gaseous concentrations of $NH_{3(g)}$, $HNO_{3(g)}$, and $HCl_{(g)}$; and the ambient RH and temperature (Fountoukis et al., 2009). The $PM_{2.5}$ ionic concentrations were measured by a Particle Into Liquid Sampler (PILS) with a 6-min integrated sampling period and a new chromatogram begun every 17 min (Orsini et al., 2003). Gaseous concentrations of $NH_{3(g)}$ were obtained with a quantum cascade laser (QCL) spectrometer and $HNO_{3(g)}$ concentrations were deduced from the volatile nitrate (i.e., $HNO_{3(g)}+NH_4NO_{3(p)}$) concentrations acquired with the thermal dissociation-laser induced fluorescence of nitrogen oxides (TD-LIF) (Day et al., 2002; Farmer et al., 2006). More details regarding data acquisition, uncertainty analysis, and quality assurance are given by Fountoukis et al. (2009).

As shown by Fountoukis et al. (2009) and since $R_S > 2$, $\frac{\partial[\mathrm{NH}^+_{4(aq)}]}{\partial[\mathrm{Total\ H_2SO_4}]} = 2\,\mathrm{mol\,mol}^{-1}$ except at RH less than the mutual deliquescence RH of $NaNO_{3(s)}$ and $NH_4NO_{3(s)}$ (i.e., approximately 50 % RH). To investigate a more variable component of the NH_4^+-SO_4^{2-}-HSO_4^--NO_3^--Na^+-Cl^--H_2O aerosol system, the sensitivity of aerosol $NO^-_{3(aq)}$ is explored as in Fountoukis et al. (2009) (Fig. 9). The Fountoukis et al. (2009) sensitivities are calculated by backward finite difference with explicit treatment of crustal species and the possibility for aerosol species to condense into solid salts. ANISORROPIA evaluates the same input by treating the crustal species $Mg_{(p)}$ and $K_{(p)}$ as equivalent moles of sodium based on ionic charge (Moya et al., 2001) and $Ca_{(p)}$ as insoluble $CaSO_{4(s)}$. Additionally, aerosol are assumed to be deliquesced, as is common in CTMs and leads to minor differences (Fountoukis et al., 2009). In an environment with excess $NH_{3(g)}$, $\frac{\partial[NO^-_{3(aq)}]}{\partial[\text{Total } HNO_3]}$ is expected to be 1 mol mol^{-1} unless insufficient aerosol water is present to absorb the additional $HNO_{3(g)}$. ANISORROPIA produces this expected sensitivity (Fig. 9, green asterisks) and with less scatter than the backward finite difference sensitivities given by Fountoukis et al. (2009). The greater scatter about the polynomial fit line for the F09 sensitivities is expected due to the limited accuracy of the finite difference method (Sect. 3.2). Furthermore, backward finite difference sensitivities exceed the expected value of 1 mol mol^{-1} for RH greater than 50 %, which ANISORROPIA more accurately represents. Complementary to this sensitivity are the values of $\frac{\partial[NO^-_{3(aq)}]}{\partial[\text{Total } NH_3]}$ and $\frac{\partial[NO^-_{3(aq)}]}{\partial[\text{Total } H_2SO_4]}$, which are expected to be zero. Again, reduced scatter above 50 % RH is evident for ANISORROPIA results. Below 50 % RH, the adjoint-based $\frac{\partial[NO^-_{3(aq)}]}{\partial[\text{Total } H_2SO_4]}$ values remain stoichiometrically realistic but exhibit increased scatter; these points correspond to stoichiometrically unrealistic $\frac{\partial[NO^-_{3(aq)}]}{\partial[\text{Total } HCl]}$ values, which could be identified and treated in a CTM adjoint implementation. The backward finite difference results for $\frac{\partial[NO^-_{3(aq)}]}{\partial[\text{Total } NH_3]}$ are significantly different than the central finite difference results with the same perturbation size, which align much more closely with ANISORROPIA $\frac{\partial[NO^-_{3(aq)}]}{\partial[\text{Total } NH_3]}$ values for 30–50 % RH (not shown). ANISORROPIA reveals that aerosol nitrate in Mexico City is primarily sensitive to the addition of $HNO_{3(g)}$, a conclusion congruent with the findings of Fountoukis et al. (2009).

5 Conclusions

The increasing measurements of aerosol composition from field campaigns and observations of aerosol precursor concentrations from satellites provide a substantial opportunity to advance the predictive capabilities of CTMs. One efficient method of gleaning valuable information from these data is to solve the inverse problem by applying the adjoint method to optimize emissions parameters, initial conditions, or boundary conditions of the CTM. Specifically, with an adjoint, the computational cost of optimization no longer scales with the number of parameters being optimized, which is essential for spatially and temporally variable aerosol precursor emissions. Furthermore, receptor-oriented sensitivity analysis, possible only with model adjoints, elucidates the relative impacts of emissions sources on air quality, human health, and climate metrics with temporal and spatial resolution.

This work presents the development and independent applications of ANISORROPIA, the adjoint of the thermodynamic aerosol model ISORROPIA for the Na^+-SO_4^{2-}-HSO_4^--NH_4^+-NO_3^--Cl^--H_2O aerosol system. Development involved modification of the forward model code and application of the automatic differentiation tool, TAPENADE (Hascoët and Pascual, 2004). Verification of ANISORROPIA required development of a complex variable version of ISORROPIA and evaluation against sensitivities produced by it, which are more reliable than the finite difference method. Further development of ANISORROPIA will extend its capacity to treat the crustal species included in ISORROPIA II (Mg^{2+}, Ca^{2+}, and K^+) as well as the reverse mode execution for the purpose of calculating dynamic equilibrium. ANISORROPIA is used to reveal the sensitivity regimes of aerosol ammonium to sulfate and fine mode, dry aerosol mass to sulfate for a wide range of atmospherically relevant conditions. ANISORROPIA is employed to characterize the sensitivity regimes of the distinct urban air masses of Atlanta and Mexico City. Receptor-oriented sensitivity analysis with CTM adjoints including ANISORROPIA shall be useful for investigating the relative contribution of specific emissions sources to radiative forcing and air quality. Within the adjoints of regional and global CTMs, ANISORROPIA can provide the ability to trace the impact of the major components of inorganic aerosol and their precursors back to the emissions source. Finally, ANISORROPIA enables assimilation of observations of inorganic aerosol precursor and aerosol concentrations in an inverse modeling framework.

Acknowledgements. SLC was supported by an NSF Graduate Research Fellowship, a Georgia Tech Institute Fellowship, and an Eastman Chemical Summer Graduate Fellowship. DKH acknowledges support from NASA Applied Sciences Program. AH acknowledges support from the National Sciences and Engineering Research Council of Canada. This work was partially funded by ConocoPhillips Company, the American Petroleum Institute, and US EPA STAR Grant RD-833866. Its contents are solely the responsibility of the grantee and do not necessarily represent the official views of the US EPA. Further, US EPA does not endorse the purchase of any commercial products or services mentioned in the publication.

References

Amundson, N. R., Caboussat, A., He, J. W., Martynenko, A. V., Savarin, V. B., Seinfeld, J. H., and Yoo, K. Y.: A new inorganic atmospheric aerosol phase equilibrium model (UHAERO), Atmos. Chem. Phys., 6, 975–992, doi:10.5194/acp-6-975-2006, 2006. 23477

Ansari, A. and Pandis, S.: Response of inorganic PM to precursor concentrations, Environ. Sci. Technol., 32, 2706–2714, 1998. 23471

Ansari, A. and Pandis, S.: Prediction of multicomponent inorganic atmospheric aerosol behavior, Atmos. Environ., 33, 745–757, 1999a. 23477

Ansari, A. and Pandis, S.: An analysis of four models predicting the partitioning of semivolatile inorganic aerosol components, Aerosol Sci. Technol., 31, 129–153, 1999b. 23477

Bartholomew-Biggs, M.: Using Forward Accumulation for Automatic Differentiation of Implicitly-Defined Functions, Comp. Optim. App., 9, 65–84, 1998. 23481

Bessagnet, B., Hodzic, A., Vautard, R., Beekmann, M., Cheinet, S., Honoré, C., Liousse, C., and Rouil, L.: Aerosol modeling with CHIMERE-preliminary evaluation at the continental scale, Atmos. Environ., 38, 2803–2817, 2004. 23474

Bey, I., Jacob, D., Yantosca, R., Logan, J., Field, B., Fiore, A., Li, Q., Liu, H., Mickley, L., and

Schultz, M.: Global modeling of tropospheric chemistry with assimilated meteorology- Model description and evaluation, J. Geophys. Res., 106, 23073–23095, 2001. 23474

Binkowski, F. and Roselle, S.: Models-3 Community Multiscale Air Quality (CMAQ) model aerosol component – 1. Model description, J. Geophys. Res., 108, 4183–4201, 2003. 23473, 23477, 23478

Byun, D. and Schere, K.: Review of the Governing Equations, Computational Algorithms, and Other Components of the Models-3 Community Multiscale Air Quality (CMAQ) Modeling System, Appl. Mechan. Rev., 59, 51–77, 2006. 23474, 23486

Capaldo, K., Pilinis, C., and Pandis, S.: A computationally efficient hybrid approach for dynamic gas/aerosol transfer in air quality models, Atmos. Environ., 21, 3617–3627, 2000. 23478

Carmichael, G., Tang, Y., Kurata, G., Uno, I., Streets, D., Woo, J.-H., Huang, H., Yienger, J., Lefer, B., Shetter, R., Blake, D., Atlas, E., Fried, A., Apel, E., Eisele, F., Cantrell, C., Avery, M., Barrick, J., Sachse, G., Brune, W., Sandholm, S., Kondo, Y., Singh, H., Talbot, R., Bandy, A., Thorton, D., Clarke, A., and Heikes, B.: Regional-scale chemical transport modeling in support of the analysis of observations obtained during the TRACE-P experiment, J. Geophys. Res., 108(D21), 8823–8851, doi:10.1029/2002JD003117, 2003. 23473, 23474

Chai, T., Carmichael, G. R., Sandu, A., Tang, Y., and Daescu, D. N.: Chemical data assimilation of Transport and Chemical Evolution over the Pacific (TRACE-P) aircraft measurements, J. Geophys. Res., 111, D02301, doi:10.1029/2005JD005883, 2006. 23472

Clegg, S., Brimblecombe, P., and Wexler, A.: Thermodynamic Model of the System H^+ NH_4^+ Na^+ SO_4^2– NO_3^- Cl^- H_2O at 298.15 K, J. Phys. Chem. A, 102, 2155–2171, 1998. 23477

Dassios, K. and Pandis, S.: The mass accommodation coefficient of ammonium nitrate aerosol, Atmos. Environ., 33, 2993–3003, 1999. 23477

Day, D. A., Wooldridge, P., Dillon, M., Thornton, J., and Cohen, R.: A thermal dissociation laser-induced fluorescence instrument for in situ detection of NO_2, peroxy nitrates, alkyl nitrates, and HNO_3, J. Geophys. Res., 107(D6), 4046, doi:10.1029/2001JD000779, 2002. 23490

Dubovik, O., Lapyonok, T., Kaufman, Y. J., Chin, M., Ginoux, P., Kahn, R. A., and Sinyuk, A.: Retrieving global aerosol sources from satellites using inverse modeling, Atmos. Chem. Phys., 8, 209–250, doi:10.5194/acp-8-209-2008, 2008. 23473, 23476

Dunker, A. M.: The decoupled direct method for calculating sensitivity coefficients in chemical kinetics, J. Chem. Phys., 81(5), 2385–2393, 1984. 23472

Edgerton, E., Hartsell, B., Saylor, R., Jansen, J., Hansen, D., and Hidy, G.: The Southeastern Aerosol Research and Characterization Study, Part 3: Continuous measurements of fine particulate matter mass and composition, J. Air Waste Manag. Assoc., 56, 1325–1341, 2006. 23489

Elbern, H., Schmidt, H., and Ebel, A.: Variational data assimilation for tropospheric chemistry modeling, J. Geophys. Res., 102(D13), 15967–15985, doi:10.1029/97JD01213, 1984. 23472

Elbern, H., Schmidt, H., Talagrand, O., and Ebel, A.: 4D-variational data assimilation with an adjoint air quality model for emission analysis, Environ. Model. Soft., 15, 539–548, 2000. 23472

ENVIRON: User's Guide to the Comprehensive Air Quality Model with Extensions (CAMx), Novato, California, USA, 1.10 edn., 1997. 23474

ENVIRON: Comprehensive Air Quality Model with extensions User's Guide, Novato, California, USA, 5.3 edn., 2010. 23474

EPA, U. S.: Air Quality Criteria for Particulate Matter, National Center for Environmental Assessment – RTP Office, Office of Research and Development, EPA/600/P-99/002aF, 2004. 23470

Farmer, D. K., Wooldridge, P. J., and Cohen, R. C.: Application of thermal-dissociation laser induced fluorescence (TD-LIF) to measurement of HNO_3, $\sum$alkyl nitrates, $\sum$peroxy nitrates, and NO_2 fluxes using eddy covariance, Atmos. Chem. Phys., 6, 3471–3486, doi:10.5194/acp-6-3471-2006, 2006. 23490

Fisher, M. and Lary, D. J.: Lagrangian four-dimensional variational data assimilation of chemical species, Q. J. Roy Meteorol. Soc., 121, 1681–1704, 1995. 23472

Forster, P., Ramaswamy, V., Artaxo, P., Berntsen, T., Betts, R., Fahey, D., Haywood, J., Lean, J., Lowe, D., and Myhre, G.: Climate Change 2007: The Physical Science Basis. Contribution of Working Group I, in: Fourth Assessment Report of the Intergovernmental Panel on Climate Change, Cambridge University Press, 2007. 23470

Fountoukis, C. and Nenes, A.: ISORROPIA II: a computationally efficient thermodynamic equilibrium model for K^+-Ca^{+2}-Mg^{+2}-NH_4^+-Na^+-SO_4^{2-}-NO_3^--Cl^--H_2O aerosols, Atmos. Chem. Phys., 7, 4639–4659, doi:10.5194/acp-7-4639-2007, 2007. 23473, 23477, 23478

Fountoukis, C., Nenes, A., Sullivan, A., Weber, R., Van Reken, T., Fischer, M., Matas, E., Moya, M., Farmer, D., and Cohen, R. C.: Thermodynamic characterization of Mexico City aerosol during MILAGRO 2006, Atmos. Chem. Phys., 9, 2141–2156, doi:10.5194/acp-9-2141-2009, 2009. 23477, 23490, 23491, 23511

Gaydos, T., Pinder, R., Koo, B., Fahey, K., Yarwood, G., and Pandis, S.: Development and application of a three-dimensional aerosol chemical transport model, PMCAMx, Atmos. Environ., 41, 2594–2611, 2007. 23471

Giles, M. and Pierce, N.: An introduction to the adjoint approach to design, Flow Turb. Comb., 65, 393–415, 2000. 23483

Griewank, A.: On automatic differentiation, in: Mathematical Programming: Recent Developments and Applications, edited by Iri, M. and Tanabe, K., 83–108, Kluwer Academic Publishers, Argonne National Laboratory, 1989. 23485

Hakami, A., Henze, D., Seinfeld, J., Chai, T., Tang, Y., Carmichael, G., and Sandu, A.: Adjoint inverse modeling of black carbon during the Asian Pacific Regional Aerosol Characterization Experiment, J. Geophys. Res., 110, D14301, doi:10.1029/2004JD005671, 2005. 23473

Hakami, A., Seinfeld, J., Chai, T., Tang, Y., Carmichael, G., and Sandu, A.: Adjoint sensitivity analysis of ozone nonattainment over the continental United States, Environ. Sci. Technol., 40, 3855–3864, 2006. 23472

Hakami, A., Henze, D., Seinfeld, J., Singh, K., and Sandu, A.: The Adjoint of CMAQ, Environ. Sci. Technol., 41(22), 7807–7817, doi:10.1021/es070944p, 2007. 23484, 23486

Hansen, D. A., Edgerton, E. S., Hartsell, B. E., Jansen, J. J., Kandasamy, N., HIDY, G. M., and Blanchard, C. L.: The Southeastern Aerosol Research and Characterization Study: Part 1-Overview, J. Air Waste Manag. Assoc., 53, 1460–1471, 2003. 23489

Hascoët, L. and Pascual, V.: TAPENADE 2.1 User's Guide, Tech. rep., INRIA Sophia Antipolis, Sophia Antipolis Cedex, 2004. 23479, 23486, 23492

Heintzenberg, J.: Fine particles in the global troposphere: A review, Tellus B, 41B, 149–160, 1989. 23471, 23477

Henze, D., Seinfeld, J., Liao, W., Sandu, A., and Carmichael, G.: Inverse modeling of aerosol dynamics: Condensational growth, J. Geophys. Res., 109, D14201, doi:10.1029/2004JD004593, 2004. 23473

Henze, D. K., Hakami, A., and Seinfeld, J. H.: Development of the adjoint of GEOS-Chem, Atmos. Chem. Phys., 7, 2413–2433, doi:10.5194/acp-7-2413-2007, 2007. 23473, 23475, 23477, 23484, 23486

Henze, D. K., Seinfeld, J. H., and Shindell, D. T.: Inverse modeling and mapping US air quality influences of inorganic $PM_{2.5}$ precursor emissions using the adjoint of GEOS-Chem, Atmos. Chem. Phys., 9, 5877–5903, doi:10.5194/acp-9-5877-2009, 2009. 23473, 23476

Huebert, B., Bates, T., Russell, P., Shi, G., Kim, Y., Kawamura, K., Carmichael, G., and Nakajima, T.: An overview of ACE-Asia: Strategies for quantifying the relationships between

Asian aerosols and their climatic impacts, J. Geophys. Res., 108, 108(D23), 8633–8653, doi:10.1029/2003JD003550, 2003. 23473

Jacobson, M.: Studying the effects of calcium and magnesium on size-distributed nitrate and ammonium with EQUISOLV II, Atmos. Environ., 33, 3635–3649, 1999. 23477

Jacobson, M., Tabazadeh, A., and Turco, R.: Simulating equilibrium within aerosols and nonequilibrium between gases and aerosols, J. Geophys. Res., 101(D4), 9079–9091, 1996. 23477

Kaminski, T., Heimann, M., and Giering, R.: A coarse grid three-dimensional global inverse model of the atmospheric transport. 2. Inversion of the transport of CO_2 in the 1980s, J. Geophys. Res., 104, 18555–18581, 1999. 23472

Kaynak, B., Hu, Y., Martin, R. V., Sioris, C. E., and Russell, A. G.: Comparison of weekly cycle of NO_2 satellite retrievals and NO_x emission inventories for the continental United States, J. Geophys. Res., 114, D05302, doi:10.1029/2008JD010714, 2009. 23476

Kelly, J. T., Bhave, P. V., Nolte, C. G., Shankar, U., and Foley, K. M.: Simulating emission and chemical evolution of coarse sea-salt particles in the Community Multiscale Air Quality (CMAQ) model, Geosci. Model Dev., 3, 257–273, doi:10.5194/gmd-3-257-2010, 2010. 23478

Kim, Y. P., Seinfeld, J. H., and Saxena, P.: Atmospheric Gas-Aerosol Equilibrium I. Thermodynamic Model, Aerosol Sci. Tech., 19, 157–181, 1993a. 23477

Kim, Y. P., Seinfeld, J. H., and Saxena, P.: Atmospheric Gas-Aerosol Equilibrium II. Analysis of Common Approximations and Activity Coefficient Calculation Methods, Aerosol Sci. Tech., 19, 182–198, 1993b. 23477, 23478

Klimont, Z. and Streets, D.: Emission inventories and projections for assessing hemispheric or intercontinental transport, in: Air Pollution Studies No. 16, edited by Keating, T. and Zuber, A., United Nations, Economic Commission for Europe, New York and Geneva, 2007. 23471

Koo, B., Dunker, A., and Yarwood, G.: Implementing the Decoupled Direct Method for Sensitivity Analysis in a Particulate Matter Air Quality Model, Environ. Sci. Technol., 41, 2847–2854, 2007. 23472

Kopacz, M., Jacob, D. J., Henze, D. K., Heald, C. L., Streets, D. G., and Zhang, Q.: Comparison of adjoint and analytical Bayesian inversion methods for constraining Asian sources of carbon monoxide using satellite (MOPITT) measurements of CO columns, J. Geophys. Res., 114, D04305, doi:10.1029/2007JD009264, 2009. 23472

Kopacz, M., Mauzerall, D. L., Wang, J., Leibensperger, E. M., Henze, D. K., and Singh, K.: Origin and radiative forcing of black carbon transported to the Himalayas and Tibetan Plateau, Atmos. Chem. Phys., 11, 2837–2852, doi:10.5194/acp-11-2837-2011, 2011. 23473

Kukkonen, J., Balk, T., Schultz, D. M., Baklanov, A., Klein, T., Miranda, A. I., Monteiro, A., Hirtl, M., Tarvainen, V., Boy, M., Peuch, V.-H., Poupkou, A., Kioutsioukis, I., Finardi, S., Sofiev, M., Sokhi, R., Lehtinen, K., Karatzas, K., San José, R., Astitha, M., Kallos, G., Schaap, M., Reimer, E., Jakobs, H., and Eben, K.: Operational, regional-scale, chemical weather forecasting models in Europe, Atmos. Chem. Phys. Discuss., 11, 5985-6162, doi:10.5194/acpd-11-5985-2011, 2011. 23472

Lamb, R., Chen, W., and Seinfeld, J.: Numerico-Empirical Analyses of Atmospheric Diffusion Theories, J. Atmosph. Sci., 32, 1794–1807, 1975. 23472

Lantoine, G., Russell, R., and Dargent, T.: Using Multicomplex Variables for Automatic Computation of High-Order Derivatives, American Astronautical Society/American Institute of Aeronautics and Astronautics Space Flight Mechanics Meeting, San Diego, California, USA, 14–17 February 2010, Paper AAS 10-218, 2010. 23483

Lyness, J. and Moler, C.: Numerical differentiation of analytic functions, SIAM J. Num. Anal., 4(2), 202–210, 1967. 23483

Malm, W. C., Sisler, J. F., Huffman, D., Eldred, R. A., and Cahill, T. A.: Spatial and seasonal trends in particle concentration and optical extinction in the United States, J. Geophys. Res., 99, 1347–1370, 1994. 23473

Marchuk, G.: Numerical solution of the problem of dynamics of atmosphere and ocean, Gidrometeoizdat, Leningrad, 1974. 23472

Martien, P. and Harley, R.: Adjoint sensitivity analysis for a three-dimensional photochemical model: Application to Southern California, Environ. Sci. Technol., 40, 4200–4210, 2006. 23472

Martien, P. T., Harley, R. A., and Cacuci, D. G.: Adjoint Sensitivity Analysis for a Three-Dimensional Photochemical Model: Implementation and Method Comparison, Environ. Sci. Technol., 40, 2663–2670, 2006. 23484

Mendoza-Dominguez, A. and Russell, A.: Estimation of emission adjustments from the application of four-dimensional data assimilation to photochemical air quality modeling, Atmos. Environ., 35, 2879–2894, 2001. 23472, 23476

Meng, Z. and Seinfeld, J.: Time scales to achieve atmospheric gas-aerosol equilibrium for volatile species, Atmos. Environ., 30(16), 2889–2900, 1996. 23477

Menut, L., Vautard, R., Beekmann, M., and Honoré, C.: Sensitivity of photochemical pollution using the adjoint of a simplified chemistry-transport model, J. Geophys. Res., 105(D12), 15379–15402, 2000. 23472

Metzger, S. and Lelieveld, J.: Reformulating atmospheric aerosol thermodynamics and hygroscopic growth into fog, haze and clouds, Atmos. Chem. Phys., 7, 3163–3193, doi:10.5194/acp-7-3163-2007, 2007. 23477

Metzger, S., Mihalopoulos, N., and Lelieveld, J.: Importance of mineral cations and organics in gas-aerosol partitioning of reactive nitrogen compounds: case study based on MINOS results, Atmos. Chem. Phys., 6, 2549–2567, doi:10.5194/acp-6-2549-2006, 2006. 23477

Molina, L. T., Madronich, S., Gaffney, J. S., Apel, E., de Foy, B., Fast, J., Ferrare, R., Herndon, S., Jimenez, J. L., Lamb, B., Osornio-Vargas, A. R., Russell, P., Schauer, J. J., Stevens, P. S., Volkamer, R., and Zavala, M.: An overview of the MILAGRO 2006 Campaign: Mexico City emissions and their transport and transformation, Atmos. Chem. Phys., 10, 8697–8760, doi:10.5194/acp-10-8697-2010, 2010 23490

Moya, M., Ansari, A., and Pandis, S. N.: Partitioning of nitrate and ammonium between the gas and particulate phases during the 1997 IMADA-AVER study, Atmos. Environ., 1791–1804, 2001. 23491

Müller, J.-F. and Stavrakou, T.: Inversion of CO and NO_x emissions using the adjoint of the IMAGES model, Atmos. Chem. Phys., 5, 1157–1186, doi:10.5194/acp-5-1157-2005, 2005. 23472

Napelenok, S., Cohan, D., Hu, Y., and Russell, A.: Decoupled direct 3D sensitivity analysis for particulate matter (DDM-3D/PM), Atmos. Environ., 40, 6112–6121, 2006. 23472

Nenes, A., Pandis, S., and Pilinis, C.: ISORROPIA: A New Thermodynamic Equilibrium Model for Multiphase Multicomponent Inorganic Aerosols, Aquat. Geochem., 4, 123–152, 1998. 23473, 23477

Nenes, A., Pandis, S., and Pilinis, C.: Continued development and testing of a new thermodynamic aerosol module for urban and regional air quality models, Atmos. Environ., 33, 1553–1560, 1999. 23471, 23473, 23477

Neuman, J., Nowak, J., Brock, C., Trainer, M., Fehsenfeld, F., Holloway, J., Hübler, G., Hudson, P., Murphy, D., Nicks Jr, D., Orsini, D., Parrish, D., Ryerson, T., Sueper, D., Sullivan, A., and Weber, R.: Variability in ammonium nitrate formation and nitric acid depletion with altitude and location over California, J. Geophys. Res., 108(D17), 4557–4569, 2003. 23489

Nowak, J., Huey, L., Russell, A., Tian, D., Neuman, J., Orsini, D., Sjostedt, S., Sullivan, A., Tanner, D., Weber, R., Nenes, A., Edgerton, E., and Fehsenfeld, F.: Analysis of urban gas phase ammonia measurements from the 2002 Atlanta Aerosol Nucleation and Real-Time Characterization Experiment (ANARChE), J. Geophys. Res., 111, D17308, doi:10.1029/2006JD007113, 2006. 23489

Orsini, D., Ma, Y., Sullivan, A., Sierau, B., Baumann, K., and Weber, R.: Refinements to the particle-into-liquid sampler (PILS) for ground and airborne measurements of water soluble aerosol composition, Atmos. Environ., 37, 1243–1259, 2003. 23490

Park, R. J., Jacob, D., Field, B., Yantosca, R., and Chin, M.: Natural and transboundary pollution influences on sulfate-nitrate-ammonium aerosols in the United States: Implications for policy, J. Geophys. Res., 109, D15204, doi:10.1029/2003JD004473, 2004. 23477

Pilinis, C., Capaldo, K., Nenes, A., and Pandis, S.: MADM-A new multicomponent aerosol dynamics model, Aerosol Sci. Tech., 32, 482–502, 2000. 23478

Pinder, R. W., Adams, P. J., and Pandis, S. N.: Ammonia Emission Controls as a Cost-Effective Strategy for Reducing Atmospheric Particulate Matter in the Eastern United States, Environ. Sci. Technol., 41, 380–386, 2007. 23471

Pye, H., Liao, H., Wu, S., Mickley, L., Jacob, D., Henze, D., and Seinfeld, J.: Effect of changes in climate and emissions on future sulfate-nitrate-ammonium aerosol levels in the United States, J. Geophys. Res., 114, D01205, doi:10.1029/2008JD010701, 2009. 23474

Resler, J., Eben, K., Jurus, P., and Liczki, J.: Inverse modeling of emissions and their time profiles, Atmos. Poll. Res., 1, 288–295, 2010. 23472

Rodgers, C.: Inverse Methods for Atmospheric Sounding, Theory and Practice, World Scientific, Singapore, 2000. 23475, 23476

Sandu, A., Daescu, D., Carmichael, G., and Chai, T.: Adjoint sensitivity analysis of regional air quality models, J. Comput. Phys., 204, 222–252, 2005a. 23472, 23473

Sandu, A., Liao, W., Carmichael, G., Henze, D., and Seinfeld, J.: Inverse Modeling of Aerosol Dynamics Using Adjoints: Theoretical and Numerical Considerations, Aerosol Sci. Tech., 39, 677–694, 2005b. 23473

Sasaki, Y.: An objective analysis based on the variational method., J. Met. Soc. Jap., 36, 77–88, 1958. 23472

Saxena, P., Belle Hudischewskyj, A., Seigneur, C., and Seinfeld, J.: A comparative study of equilibrium approaches to the chemical characterization of secondary aerosols, Atmos. Environ., 20, 1471–1483, 1986. 23477

Schaap, M., Timmermans, R. M. A., Roemer, M., Boersen, G. A. C., Builtjes, P. J. H., Sauter, F. J., Velders, G. J. M., and Beck, J. P.: The LOTOS-EUROS model: description, validation and latest developments, Int. J. Environ. Pollution, 32, 270–290, 2008. 23474

Schmidt, H., Derognat, C., Vautard, R., and Beekmann, M.: A comparison of simulated and observed ozone mixing ratios for the summer of 1998 in Western Europe, Atmos. Environ., 35, 6277–6297, 2001. 23474

Seinfeld, J. H. and Pandis, S. N.: Atmospheric Chemistry and Physics: From Air Pollution to Climate Change, John Wiley, New York, USA, 2nd edn., 2006. 23477, 23487

Seinfeld, J. H., Carmichael, G. R., Arimoto, R., Conant, W. C., Brechtel, F. J., Bates, T. S., Cahill, T. A., Clarke, A. D., Doherty, S. J., Flatau, P. J., Huebert, B. J., Kim, J., Markowicz, K. M., Quinn, P. K., Russell, L. M., Russell, P. B., Shimizu, A., Shinozuka, Y., Song, C. H., Tang, Y., Uno, I., Vogelmann, A. M., Weber, R. J., Woo, J.-H., and Zhang, X. Y.: ACE-ASIA: Regional Climatic and Atmospheric Chemical Effects of Asian Dust and Pollution, Bull. Amer. Met. Soc., 85, 367–380, 2004. 23473

Sekiyama, T. T., Tanaka, T. Y., Shimizu, A., and Miyoshi, T.: Data assimilation of CALIPSO aerosol observations, Atmos. Chem. Phys., 10, 39–49, doi:10.5194/acp-10-39-2010, 2010. 23473

Shindell, D., Lamarque, J.-F., Unger, N., Koch, D., Faluvegi, G., Bauer, S., Ammann, M., Cofala, J., and Teich, H.: Climate forcing and air quality change due to regional emissions reductions by economic sector, Atmos. Chem. Phys., 8, 7101–7113, doi:10.5194/acp-8-7101-2008, 2008. 23471

Shindell, D. T., Faluvegi, G., Koch, D. M., Schmidt, G. A., Unger, N., and Bauer, S. E.: Improved Attribution of Climate Forcing to Emissions, Science, 326, 716–718, 2009. 23471

Solomon, P. A., Chameides, W., Weber, R., Middlebrook, A., Kiang, C. S., Russell, A. G., Butler, A., Turpin, B., Mikel, D., Scheffe, R., Cowling, E., Edgerton, E., St John, J., Jansen, J., McMurry, P., Hering, S., and Bahadori, T.: Overview of the 1999 Atlanta Supersite Project, J. Geophys. Res., 108(D7), 8413–8437, doi:10.1029/2001JD001458, 2003. 23489

Squire, W. and Trapp, G.: Using complex variables to estimate derivatives of real functions, SIAM Rev., 40, 110–112, 1998. 23483

Streets, D. G., Zhang, Q., Wang, L., He, K., Hao, J., Wu, Y., Tang, Y., and Carmichael, G. R.: Revisiting China's CO emissions after the Transport and Chemical Evolution over the Pacific (TRACE-P) mission: Synthesis of inventories, atmospheric modeling, and observations, J. Geophys. Res., 111, D14306, doi:10.1029/2006JD007118, 2006. 23476

Talagrand, O.: On the mathematics of data assimilation, Tellus, 33(4), 321–339, 1981. 23472

Talagrand, O. and Courtier, P.: Variational assimilation of meteorological observations with the adjoint vorticity equation. 1. Theory, Q. J. Roy. Meteorol. Soc., 113, 1311–1328, 1987. 23472

Uno, I., Yumimoto, K., Shimizu, A., Hara, Y., Sugimoto, N., Wang, Z., Liu, Z., and Winker, D. M.: 3D structure of Asian dust transport revealed by CALIPSO lidar and a 4DVAR dust model, Geophys. Res. Lett., 35, L06803, doi:10.1029/2007GL032329, 2008. 23473

Vayenas, D., Takahama, S., Davidson, C., and Pandis, S.: Simulation of the thermodynamics and removal processes in the sulfate-ammonia-nitric acid system during winter: Implications for PM2.5 control strategies, J. Geophys. Res., 110, D07S14, doi:10.1029/2004JD005038, 2005. 23471

Vogel, B., Vogel, H., Bäumer, D., Bangert, M., Lundgren, K., Rinke, R., and Stanelle, T.: The comprehensive model system COSMO-ART- Radiative impact of aerosol on the state of the atmosphere on the regional scale, Atmos. Environ., 9, 8661–8680, 2009. 23474

Vukićević, T. and Hess, P.: Analysis of tropospheric transport in the Pacific Basin using the adjoint technique, J. Geophys. Res., 105(D6), 7213–7230, 2000. 23472

West, J., Pilinis, C., Nenes, A., and Pandis, S.: Marginal direct climate forcing by atmospheric aerosols, Atmos. Environ., 32, 2531–2542, 1998. 23471

West, J., Ansari, A., and Pandis, S.: Marginal $PM_{2.5}$: Nonlinear aerosol mass response to sulfate reductions in the Eastern United States, J. Air Waste Manag. Assoc., 49, 1415–1424, 1999. 23471

Yumimoto, K., Uno, I., Sugimoto, N., Shimizu, A., and Satake, S.: Adjoint inverse modeling of dust emission and transport over East Asia, Geophys. Res. Lett., 34, L08806, doi:10.1029/2006GL028551, 2007. 23473

Yumimoto, K., Uno, I., Sugimoto, N., Shimizu, A., Liu, Z., and Winker, D. M.: Adjoint inversion modeling of Asian dust emission using lidar observations, Atmos. Chem. Phys., 8, 2869–2884, doi:10.5194/acp-8-2869-2008, 2008. 23473

Zaveri, R., Easter, R., and Peters, L.: A computationally efficient multicomponent equilibrium solver for aerosols (MESA), J. Geophys. Res., 110, D24203, doi:10.1029/2004JD005618, 2005. 23477

Zhang, L., Constantinescu, E., Sandu, A., Tang, Y., Chai, T., Carmichael, G., Byun, D., and Olaguer, E.: An adjoint sensitivity analysis and 4D-Var data assimilation study of Texas air quality, Atmos. Environ., 42, 5787–5804, 2008. 23472

Zhang, W., Capps, S., Hu, Y., Nenes, A., Napelenok, S., and Russell, A.: Development of High-Order DDM Sensitivity Analysis for Particulate Matter in Multidimensinal Air Quality Models, Geosci. Model Dev. Discuss., in review, 2011. 23472

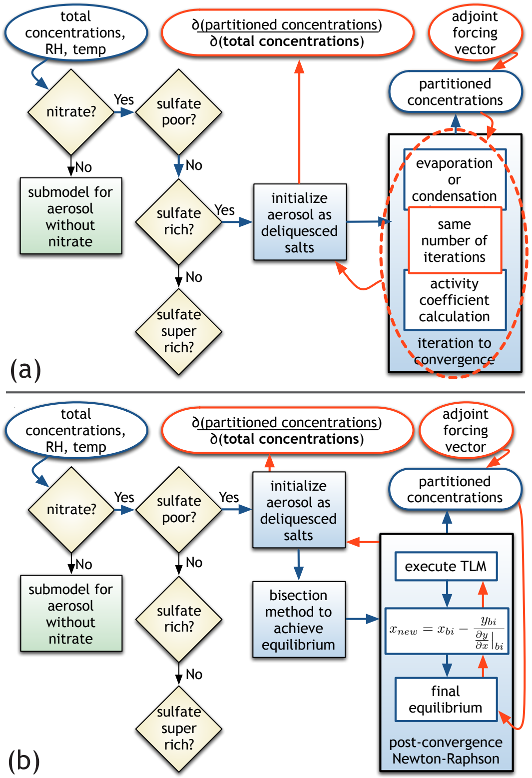

Fig. 1. Algorithmic flowchart of ISORROPIA forward (blue) and adjoint (orange) calculations. **(a)** The acidic aerosol solution algorithm is given for the cases where the molar ratio of total ammonia (i.e., [Total Ammonia] = $[\mathrm{NH}^+_{4(\mathrm{aq})}] + [\mathrm{NH}_{3(\mathrm{g})}]$) to total sulfate is less than two ($R_S < 2$); **(b)** for $R_S \geq 2$, the neutralized aerosol solution algorithm is shown.

Title Page
Abstract | Introduction
Conclusions | References
Tables | Figures
◀| |▶
◀ ▶
Back | Close
Full Screen / Esc
Printer-friendly Version
Interactive Discussion

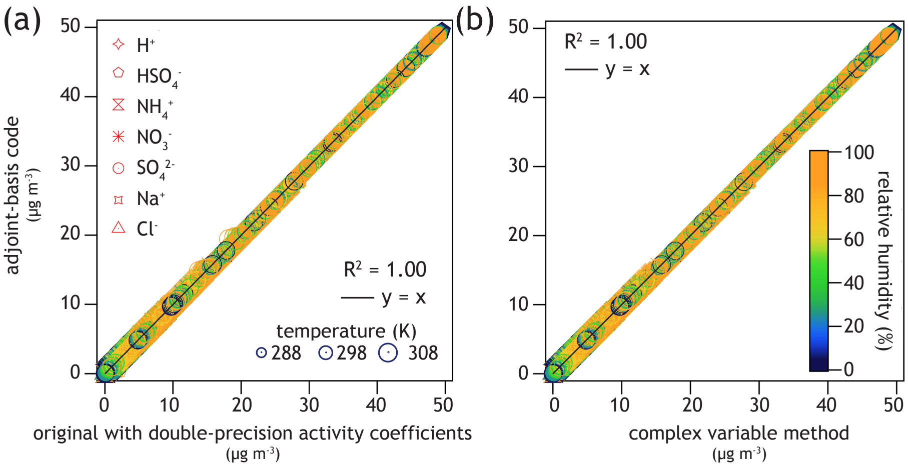

Fig. 2. Evaluation of concentrations of aqueous species in µg m^{-3} produced by forward model augmented for adjoint development against **(a)** ISORROPIA v.2.1 with a modified double-precision activity coefficient module and **(b)** the complex variable method version of ISORROPIA v.2.1 with double-precision activity coefficient module. The atmospherically relevant range of concentrations, RH, and temperature evaluated is given in Sect. 3 of the text. In each case, the intercept and slope of the linear regression were negligibly different than 0 and 1, respectively.

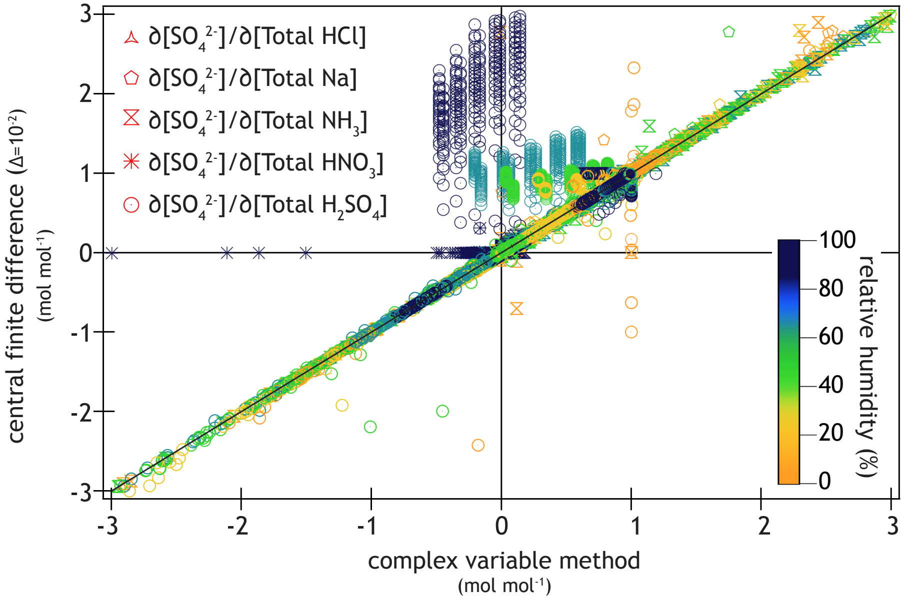

Fig. 3. Sensitivities from the central finite difference method with a delta value of 10^{-2} compared against sensitivities from the complex variable method with a perturbation of $10^{-18}i$. The line $y = x$ is plotted for reference (solid black). Deviations from stoichiometric expectations in finite difference sensitivities revealed that the finite difference approach would not suffice to evaluate ANISORROPIA sensitivities.

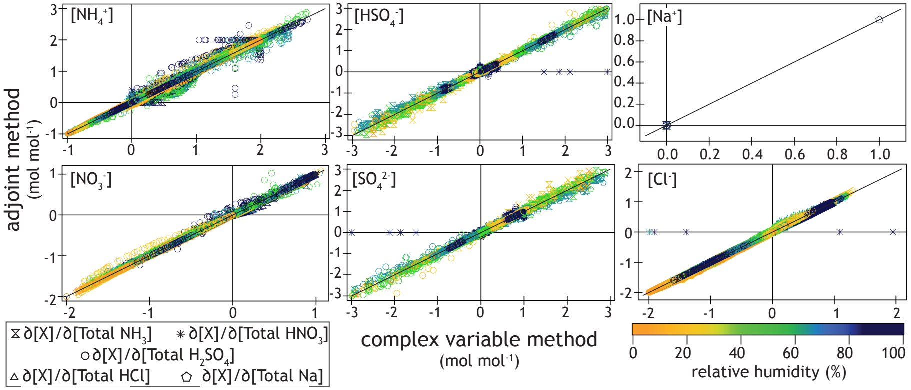

Fig. 4. The sensitivities of aqueous species with respect to the total amount of each aerosol species (mol mol^{-1}) from ANISORROPIA are shown against those from CVM for the range of aerosol precursor concentrations, temperature, and RH outlined in the text (Sect. 3).

Title Page
Abstract
Introduction
Conclusions
References
Tables
Figures
◀▮
▶▮
◀
▶
Back
Close
Full Screen / Esc
Printer-friendly Version
Interactive Discussion

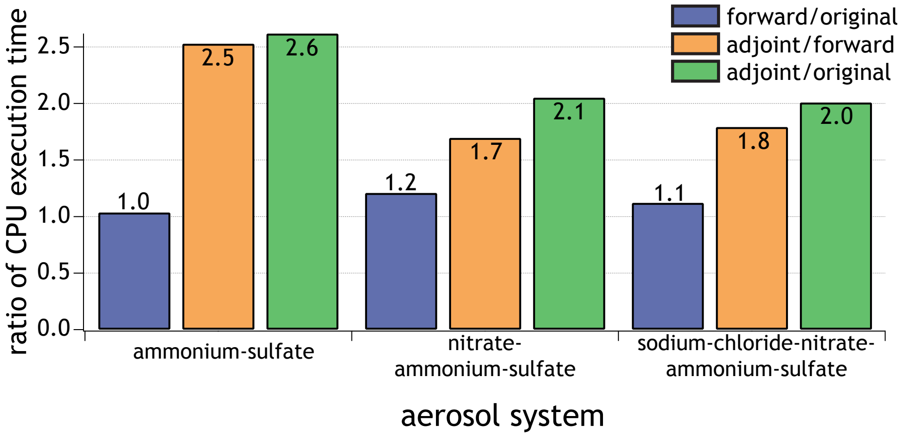

Fig. 5. The ratios comparing CPU execution time for the calculations of ANISORROPIA forward concentrations (forward), ANISORROPIA adjoint sensitivities (adjoint), and ISORROPIA v.2.1 forward concentrations (original) are shown. Experiments were designed to elucidate the ratios for each of the aerosol systems treated in ANISORROPIA (SO_4^{2-}-HSO_4^--NH_4^+-H_2O; NO_3^--SO_4^{2-}-HSO_4^--NH_4^+-H_2O; Na^+-Cl^--NO_3^--SO_4^{2-}-HSO_4^--NH_4^+-H_2O). The forward/original comparison reveals the additional time required to evaluate activity coefficients in double precision and to execute routines added where needed for adjoint traceability (e.g., post-convergence Newton-Raphson).

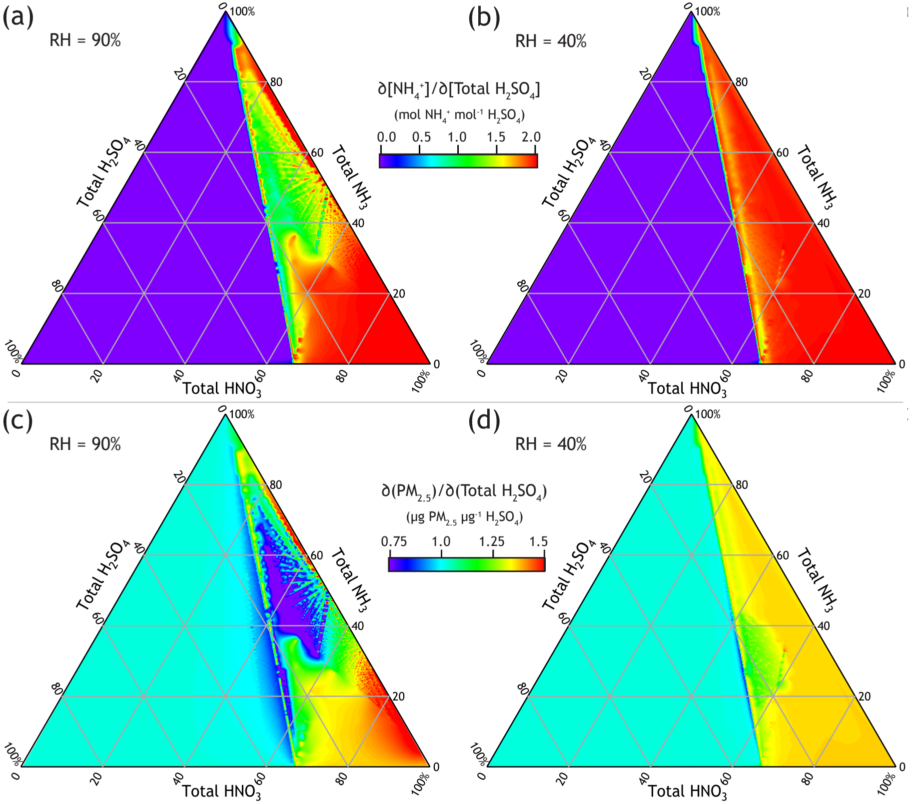

Fig. 6. ANISORROPIA-produced $\frac{\partial[NH^+_{4(aq)}]}{\partial[\mathrm{Total}\,H_2SO_4]}$ (mol mol^{-1}) **(a,b)** and $\frac{\partial(PM_{2.5,dry})}{\partial(\mathrm{Total}\,H_2SO_4)}$ (µg µg^{-1}) **(c,d)** for the NH_4^+-SO_4^{2-}-HSO_4^--NO_3^--H_2O aerosol system at RH of 90 % **(a,c)** and 40 % **(b,d)** and a temperature of 300 K. The axes convey the percent a total species (adjacent label) contributes to the molar composition of the system.

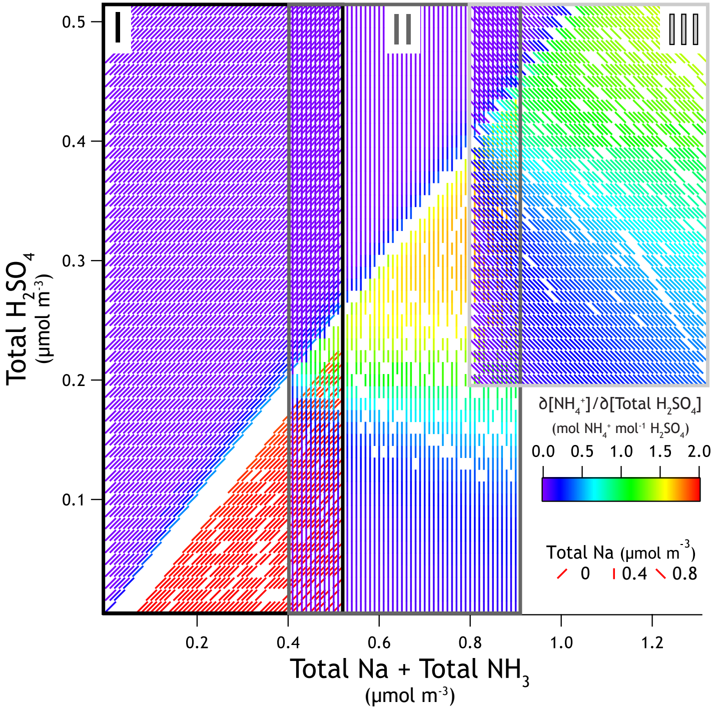

Fig. 7. ANISORROPIA-produced $\frac{\partial[\mathrm{NH}_{4(aq)}^{+}]}{\partial[\mathrm{Total\ H_2SO_4}]}$ (mol mol^{-1}) for the NH_4^+-SO_4^{2-}-HSO_4^--NO_3^--Na^+-Cl^--H_2O aerosol system at a RH of 40 % and a temperature of 300 K. The total HCl is 0.8 µmol m^{-3}, and the total HNO_3 is 0.01 µmol m^{-3}. Region I corresponds to 0 µmol m^{-3} of total Na, region II to 0.4 µmol m^{-3} of total Na, and region III to 0.8 µmol m^{-3} of total Na. Note the transition in sensitivity at a ratio of 2 moles of positive ions (total NH_3 + Na) to 1 mole of total H_2SO_4 ($R_S = 2$). The increasing gradient from left to right in Regions II and III demonstrates the initial effectiveness of $Na_{(aq)}^+$ to neutralize $SO_{4(aq)}^{2-}$ (i.e., low $\frac{\partial[\mathrm{NH}_{4(aq)}^{+}]}{\partial[\mathrm{Total\ H_2SO_4}]}$) and the increasing role of $NH_{4(aq)}^+$ in neutralization.

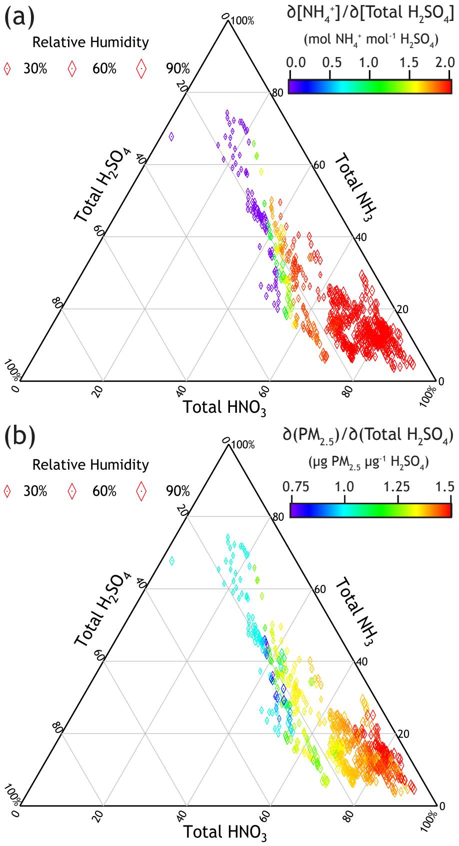

Fig. 8. ANARChE data processed with ANISORROPIA reveal Atlanta $\frac{\partial[\mathrm{NH}^+_{4(aq)}]}{\partial[\mathrm{Total\,H_2SO_4}]}$ (mol mol^{-1}) **(a)** and $\frac{\partial(\mathrm{PM_{2.5,dry}})}{\partial(\mathrm{Total\,H_2SO_4})}$ (µg µg^{-1}) **(b)** in July–August 2002. RH ranges from 25 %–99 % and temperature from 293 K to 310 K.

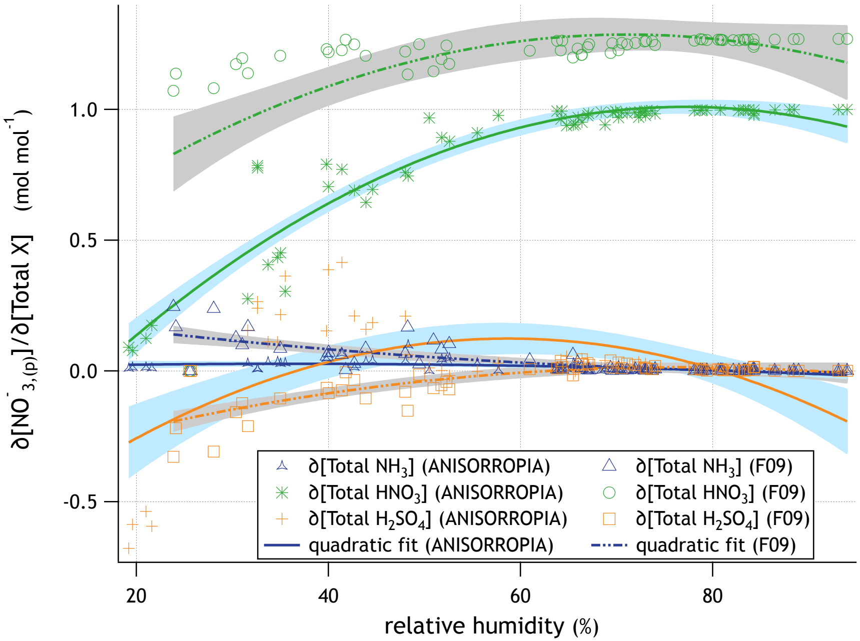

Fig. 9. The ANISORROPIA-produced $\frac{\partial[\mathrm{NO}^-_{3(aq)}]}{\partial[\mathrm{Total\,HNO_3}]}$, $\frac{\partial\mathrm{NO}^-_{3(aq)}}{\partial[\mathrm{Total\,NH_3}]}$, and $\frac{\partial\mathrm{NO}^-_{3(aq)}}{\partial[\mathrm{Total\,H_2SO_4}]}$ values are plotted alongside backward finite difference sensitivities from Fountoukis et al. (2009) (F09). The quadratic fits to the senstivity data are shown to direct the eye with the 95 % confidence interval given by the shaded bands about the fit lines. Solid lines and light blue shading correspond to ANISORROPIA sensitivities; dashed lines and gray shading correspond to F09 sensitivities. With the exception of the fit about $\frac{\partial\mathrm{NO}^-_{3(aq)}}{\partial[\mathrm{Total\,H_2SO_4}]}$, ANISORROPIA has tighter bands than F09, indicating less scatter in the results due to the direct computation of sensitivity about the desired input. ANISORROPIA characterizes the sensitivity of Mexico City aerosol nitrate similarly to the full forward model employed by F09.